APPLIED PHYSICS LETTERS **110**, 031901 (2017)

Flexible amorphous metal films with high stability

M. Liu, C. R. Cao, Y. M. Lu, W. H. Wang, and H. Y. Bai[a)]
Institute of Physics, Chinese Academy of Sciences, Beijing 100190, People's Republic of China

(Received 14 October 2016; accepted 4 January 2017; published online 17 January 2017)

We report the formation of amorphous $Cu_{50}Zr_{50}$ films with a large-area of more than 100 cm^2. The films were fabricated by ion beam assisted deposition with a slow deposition rate at moderate temperature. The amorphous films have markedly enhanced thermal stability, excellent flexibility, and high reflectivity with atomic level smoothness. The multifunctional properties of the amorphous films are favorites in the promising applications of smart skin or wearable devices. The method of preparing highly stable amorphous metal films by tuning the deposition rate instead of deposition temperature could pave a way for exploring amorphous metal films with unique properties. *Published by AIP Publishing*. [http://dx.doi.org/10.1063/1.4974153]

Metallic glasses (MGs), which quenched from liquids with high cooling rates, have no long-range ordered periodic microstructures and lie in the metastable states in the potential energy landscape.[1,2] The MGs with unique functional and engineering properties, such as high strength and high corrosion resistance, could be potential structural and functional materials.[3–6] Amorphous metal films adopt these unique characteristics from their bulk form and show great potential in many areas.[7–10] However, the thermal stability, good flexibility, low surface roughness, and large area are also essential requirements for the practical applications of these films, such as wearing[11] and smart skin.[12] The metastable nature of amorphous materials makes them be prone to aging and crystallization, which will severely deteriorate the useful properties. The amorphous metal films with ultrahigh thermal stability have also been prepared by magnetron sputtering deposition[13,14] and pulsed laser deposition.[15] The higher deposition substrate temperature (0.7–0.85 T_g (Refs. 13, 14, and 16) or about several hundred degrees) was found to be necessary to obtain highly stable amorphous films because the surface atomic mobility during the deposition process is the key factor for the ultrastable amorphous film formation.[15,17] The glass transition temperature T_g and onset of crystallization temperature T_x could be improved efficiently by applying higher substrate temperature. However, these stable amorphous metal films are usually brittle and lack flexibility, which is suggested to be induced by the heating process during deposition.

In this letter, we report a scheme of ion beam assisted deposition (IBAD) to prepare the highly thermal stable amorphous metal films. The onset of crystallization temperature of the fabricated amorphous $Cu_{50}Zr_{50}$ films can be increased by more than 59 K compared to that of the normal ribbon. These amorphous films with a large area over 100 cm^2 also exhibit good flexibility, high hardness, and good reflectivity with atomic level smoothness. The current deposition method could be more efficient for the preparation of films with higher thermal stability and other useful properties, which are favorites for coating and smart skin research areas.

The $Cu_{50}Zr_{50}$ ingot was obtained by arc-melting the mixtures of Copper and Zirconium with 99.99% purity in a high-purity argon atmosphere. Deposition targets were prepared by melting the ingots and casting into the plate-shaped cooper mold with the dimensions of 4 cm × 6 cm. The amorphous $Cu_{50}Zr_{50}$ film deposition process was as follows: one layer of Aluminum with about 100 nm thickness was first deposited on a flat polycarbonate (PC) plate, and then the amorphous $Cu_{50}Zr_{50}$ films were deposited on the substrates mentioned above by the IBAD method. The base pressure of the deposition processes was lower than 3×10^{-4} Pa, and the argon pressure during deposition was 2.4×10^{-2} Pa. A series of amorphous films with a similar thickness of about 1 μm were fabricated by controlling ion beam currents (15, 20, 25, 30, and 40 mA). The NaOH aqueous solution (1.5 mol/l) was used to peel the films from the substrates, and then the films were soaked in deionized water to remove the impurities. The $Cu_{50}Zr_{50}$ ribbon was prepared by using a melt-spinning machine in the high purity argon atmosphere. The speed of the rotating copper wheel was kept about 100 r/s, and the argon pressure was about 20 kPa. The dimensions for the fabricated $Cu_{50}Zr_{50}$ ribbons are 1 mm in width and 40 μm in thickness.

The deposition thickness of the amorphous films with different ion beam currents was characterized by X-ray reflectometry (XRR; Rigaku SmartLab). Chemical analysis was used to determine the composition of free standing films. The result shows that the atomic ratio of Cu and Zr of the fabricated MG films was almost equals to 1:1, and impurity elements were less than 2%. The oxygen content of the films both in the amorphous and crystallized states was measured by using an oxygen and nitrogen analyzer (Baoying Technology, TC-306). The amorphous structure of the MG films was confirmed by X-ray diffraction (XRD, Bruker D8A A25) with Cu K_α radiation and high resolution transmission electron microscopy (HRTEM, Philips CM200). Thermal properties were measured by using a differential scanning calorimeter (DSC, Perkin Elmer 8000) at different heating rates (3, 20, 40, and 80 K/min) under a purified argon atmosphere. Atom force microscopy (AFM, Asylum Research MFP-3D) was utilized to characterize the surface roughness of these films on the silicon substrates. Hardness

---

[a)] Author to whom correspondence should be addressed. Electronic mail: hybai@iphy.ac.cn

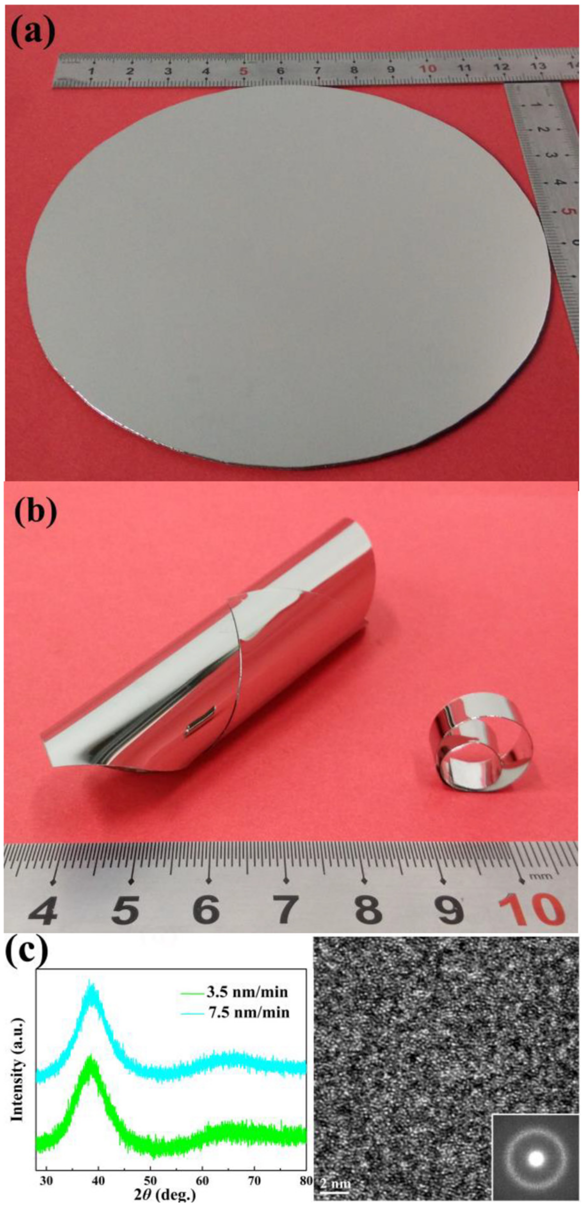

FIG. 1. (a) Image of the $Cu_{50}Zr_{50}$ film on a PC substrate with an area over 100 cm^2. (b) The $Cu_{50}Zr_{50}$ films deposited on a 0.1 mm PC substrate show high flexibility. These films were fabricated with a deposition rate of 3.5 nm/min. The films show excellent flexibility by bending into a circle shape with a diameter less than 1 centimeter, and the surface remains smooth without any visible fracture fringe. (c) X-ray diffraction patterns of free standing amorphous $Cu_{50}Zr_{50}$ films with the deposition rates of 3.5 nm/min and 7.5 nm/min. The right image shows the high resolution transmission electron microscopy image of the amorphous $Cu_{50}Zr_{50}$ film with the deposition rate of 3.5 nm/min. The inset shows the selected area electron diffraction pattern of the film.

was also measured by nanoindentation (Bruker Dimension icon with Scan Asyst) to further characterize the mechanical properties of the amorphous metal films on silica.

Figure 1(a) shows that a fabricated amorphous $Cu_{50}Zr_{50}$ film on the PC plate has a large area of over 100 cm^2 with a diameter of 12 cm, which is much larger than that of films prepared by vapor deposition and magnetron sputtering methods.[18–20] The films with large area were achieved by the IBAD with a large ion source. The amorphous nature of the fabricated films with different deposition rates was checked by XRD. There is no observable crystalline peak and no

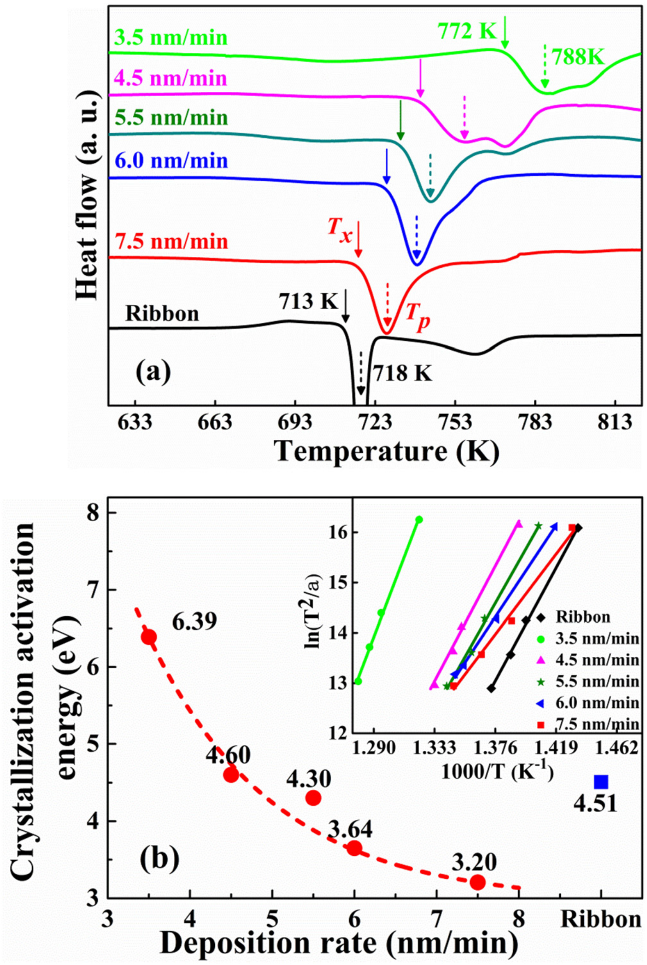

FIG. 2. (a) DSC scans at a heating rate of 20 K/min for the free standing amorphous $Cu_{50}Zr_{50}$ films and the MG ribbon. The arrows of corresponding colors represent the onset crystallization temperature, T_x, for MG films with deposition rates of 3.5, 4.5, 5.5, 6.0, and 7.5 nm/min, respectively. (b) Crystallization activation energy for $Cu_{50}Zr_{50}$ films and ribbon evaluated by using the Kissinger method. The dashed line is a guide for the eye. The inset shows the heating rate dependence of the T_x in the Kissinger coordinates. T_x is characterized with heating rates of 3, 20, 40, and 80 K/min.

crystallization phase in the HRTEM image either as shown in Fig. 1(c), confirming that the films are fully amorphous. The films have a smooth surface even after bending into a roll with a diameter less than 1 cm as shown in Fig. 1(b), which suggests that the films have high flexibility.

The thermal stability of the $Cu_{50}Zr_{50}$ MG ribbon and the free-standing $Cu_{50}Zr_{50}$ film with different deposition rates was characterized by DSC at a heating rate of 20 K/min as shown in Fig. 2(a). The glass transition temperature, T_g, has been wildly used to characterize the thermal stability of a glassy film.[13,14] However, for the ion beam deposition method, with a slow deposition rate, the atoms were deposited separately without the strong atomic correlation like that quenched from liquids, the glass transition process is not obviously distinct, and the T_g is hard to be detected in the DSC curve. Thus, the onset crystallization temperature, T_x, or the position of the crystallization exothermic peak, T_p, is used to quantitatively characterize the thermal stability of the MG films. Figure 2(a) shows that the values of T_x for various amorphous metal films are much higher than that of the corresponding MG ribbon. To get rid of the impact of zirconium content loss by oxidation on

RIGHTSLINK

the change in the T_x,[21–23] the oxygen content and atomic structure at different temperatures were characterized as shown in Fig. S1 (supplementary material). The oxygen contents for these films before and after crystallization are below 0.7% (wt.). Combing these results from element analysis, it can be verified that the increase in T_x is not caused by the change in the composition and oxidization of the films, suggesting that the ion beam assisted deposition method can efficiently enhance the thermal stability of the films. With the decrease in the deposition rate, the values of T_x of the amorphous films increase, suggesting that the prepared films with a slower deposition rate tend to be more stable. The amorphous film with the lowest deposition rate of 3.5 nm/min has the highest T_x (772 K), compared with that of the ribbon (713 K); the T_p for the film (788 K) is also higher than T_p for the ribbon (718 K), further confirming that the amorphous metal films fabricated at the moderate temperature display high thermal stability.

To further investigate the thermal stability of these amorphous metal films, the crystallization activation energy, E_A, was evaluated by using the Kissinger model[24]

$$\ln\frac{T^2}{\alpha} = \frac{E_A}{kT} + C, \tag{1}$$

where T stands for T_x or T_p, α is the heating rate, k is Boltzmann's constant, and C is a constant. The crystallization activation energy for all amorphous metal films and MG ribbon was deduced by fitting the slope of the $\ln(T^2\alpha^{-1}) - T^{-1}$, as shown in the inset of Fig. 2(b). The evaluated values of E_A for the amorphous films and the value of E_A for the ribbon are shown in Fig. 2(b) for comparison. The dashed line is a guide for the eye. The value of E_A for the $Cu_{50}Zr_{50}$ ribbon (4.5 eV) is in agreement with a previous report.[25] The E_A for the amorphous films increases with the decrease in the deposition rates, and the E_A corresponding to the lowest deposition rate is almost two times larger than that of the sample with the fastest deposition rate. The enhanced E_A confirms the higher thermal stability of these films. The crystallization mechanism for MGs verified by many experiments is diffusion controlled crystallization.[26–30] It is noted that the effect of tuning deposition rates at moderate temperature is equivalent to tuning deposition temperatures.[29] At a slower deposition rate, the atoms have longer time to reach the lower energy state in the potential energy landscape during the deposition process.[30] The MGs in the lower energy state mostly have lower quantity of free volume. Limited by the free volume, the material would have lower atomic mobility, which could retard the atoms to diffuse into the crystalline phase. Besides, increased E_A could also be due to the strong interaction between atoms. Figure 3 illustrates the change in the hardness of the amorphous metal films with various deposition rates. One can see that with the decrease in the deposition rate, the hardness of these films increases, and the film with the lowest deposition rate has the highest hardness of 6.4 GPa, which increases by 10% compared with that of the amorphous film with the fastest deposition rate (5.8 GPa). The increased hardness with a slower deposition rate suggests that the atomic interaction becomes stronger. The combination of less free volume and stronger bonding between atoms could induce lower mobility of the atoms, which endues the films with higher E_A. The difference of E_A for films and ribbon further confirms the higher thermal stability of the amorphous films with a lower deposition rate. Theoretical simulations and experimental investigations in glasses show that the surface free energy barrier for atom arrangement is half of that for the bulk material.[31] Because the atoms in the surface layer tend to rearrange their positions easily compared with those interior atoms that are confined by their neighbor atoms in three dimensions, the quenched bulk MG has moderate crystallization activation energy compared with deposited films.

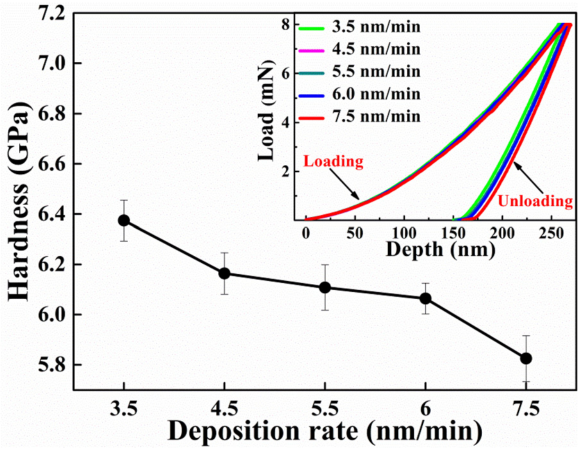

FIG. 3. The dependence of hardness on the deposition rate of amorphous $Cu_{50}Zr_{50}$ films measured by nanoindentation. The inset shows the load-depth curves of $Cu_{50}Zr_{50}$ films with different deposition rates.

The roughness of the film was characterized by AFM as shown in Fig. 4(a). The root-mean-square surface roughness of the film is 0.118 nm, which reaches the atomic scale, implying that the films have atomic level smoothness. Figure 4(b) shows the image of the films on a 0.8 mm PC plate. The film on a PC substrate has a perfect surface and shows specular reflection of the bending amorphous film ring with a 0.1 mm PC substrate. This smooth surface and enhanced hardness are contributed from the very low deposition rate because the atoms are sputtered tightly with fewer defects formed with a lower deposition rate. The high flexiblity makes these stable films easily be attached on human skin as shown in Fig. 4(c).

During the deposition process, the temperature of the substrate is kept about 370 K, which is near room temperature and far below the substrate temperature (about 0.7–0.85 T_g (Refs. 13, 14, and 16) or about several hundred degrees) in other deposition methods such as magnetron sputtering deposition[13,14] and pulsed laser deposition[15] for obtaining highly stable amorphous films. Our deposition substrate temperature is also below the soften temperature of PC. This fabrication strategy has few restrictions for the substrates; the moderate substrates including polymers can be used, and the obtained amorphous films can be featured with high thermal stability, flexibility, and markedly enhanced reflectivity with an atomic scale smooth surface. The general mechanism for obtaining highly thermal and kinetic stability has been investigated by both experiments and stimulations.[29,30] The stability of ultrastable films prepared by vapor

RIGHTSLINK

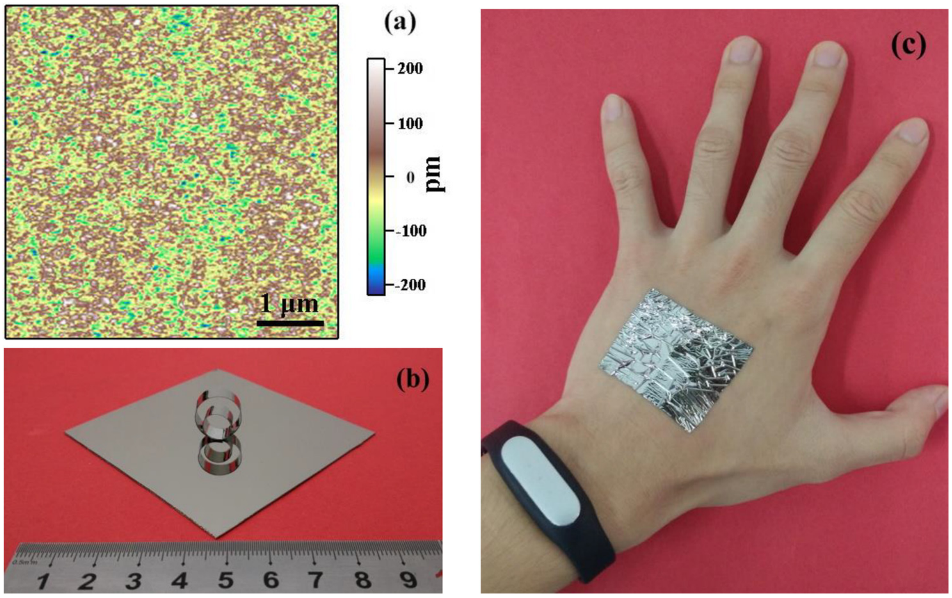

FIG. 4. (a) AFM image of the surface topography for $Cu_{50}Zr_{50}$ films with a deposition rate of 3.5 nm/min. (b) Image of $Cu_{50}Zr_{50}$ films on the PC substrates with different thicknesses. These films show specular reflection (the ring is the MG film deposited on a 0.1 mm thickness PC, and the plate is the amorphous metal film deposited on a 0.8 mm thickness PC). (c) Peeled free-standing $Cu_{50}Zr_{50}$ film with a large area could be easily (deposition rate of 3.5 nm/min) attached on skin.

deposition is attributed to a highly efficient pack process due to the lower free energy barrier and high rearrangement rate for those deposited atoms in the surface layer. By applying the vapor deposition at controlled temperature, the films could be packed with less voids compared with bulk glasses quenched from liquids. High deposition temperture is suggested to accelerate the diffusion of the atoms.[32] However, in the present method, a highly efficient packed process is achieved by the much slower atomic deposition rate (3.5 nm/min compared with 12–84 nm/min for magnetron sputtering[13,14]), and the atoms on the surface layer with fast relaxation or a diffusion rate could be densely packed for the reasonable duration without importing energy from heated substrates. The formed densely packed microstructure results in the enhanced thermal stability, higher hardness, and the atomic scale smooth surface based on the flow unit perspective of MGs.

In summary, the amorphous $Cu_{50}Zr_{50}$ films with large area were achieved by ion beam assisted deposition by tuning the deposition rates instead of deposition temperatures. These amorphous films have extraordinary thermal stability, high flexibility, and atomic level smoothness. These multifunctional features of the amorphous films make them be potentially useful for technology, such as coating for MEMS and wearing. The peeled free standing amorphous films could have promising applications in the smart skin or wearable devices. In addition, the film fabrication method that tunes the deposition rate instead of deposition temperature paves a way for the exploration of amorphous metal films with unique physical and mechanical properties.

See supplementary material for details about the X-ray diffraction patterns and oxygen content for the $Cu_{50}Zr_{50}$ film with the deposition rate of 3.5 nm/min at different temperatures.

We thank M. Gao, L. Z. Zhao, C. Wang, P. Luo, D. W. Ding, and D. Q. Zhao for insightful discussions and experimental assistance. This work was supported by the NSF of China (51571209 and 51461165101) and MOST 973 Program (No. 2015CB856800).

[1] C. A. Angell, Science **267**, 1924 (1995).
[2] P. G. Debenedetti and F. H. Stillinger, Nature **410**, 259 (2001).
[3] W. H. Wang, Adv. Mater. **21**, 4524 (2009).
[4] A. Inoue and A. Takeuchi, Acta Mater. **59**, 2243 (2011).
[5] M. Carmo, R. C. Sekol, S. Y. Ding, G. Kumar, J. Schroers, and A. D. Taylor, ACS Nano **5**, 2979 (2011).
[6] W. Chen, J. Ketkaew, Z. Liu, R. M. O. Mota, K. O'Brien, C. S. da Silva, and J. Schroers, Scr. Mater. **107**, 1 (2015).
[7] W. Diyatmika, J. P. Chu, B. T. Kacha, C.-C. Yu, and C.-M. Lee, Curr. Opin. Solid State Mater. Sci. **19**, 95 (2015).
[8] C. Zhang, Y. Wu, and L. Liu, Appl. Phys. Lett. **101**, 121603 (2012).
[9] N. Kaushik, P. Sharma, S. Ahadian, A. Khademhosseini, M. Takahashi, A. Makino, S. Tanaka, and M. Esashi, J. Biomed. Mater. Res. Part B **102**, 1544 (2014).
[10] J. P. Chu, J. C. Huang, J. S. C. Jang, Y. C. Wang, and P. K. Liaw, JOM **62**, 19 (2010).
[11] J. P. Chu, J. S. C. Jang, J. C. Huang, H. S. Chou, Y. Yang, J. C. Ye, Y. C. Wang, J. W. Lee, F. X. Liu, P. K. Liaw, Y. C. Chen, C. M. Lee, C. L. Li, and C. Rullyani, Thin Solid Films **520**, 5097 (2012).
[12] M. Shi, J. Zhang, H. Chen, M. Han, S. A. Shankaregowda, Z. Su, B. Meng, X. Cheng, and H. Zhang, ACS Nano **10**, 4083 (2016).
[13] D. P. B. Aji, H. Akihiko, F. Zhu, P. Liu, M. K. Reddy, S. X. Song, Y. H. Liu, T. Fujita, S. Kohara, and M. W. Chen, preprint arXiv:1306.1575 (2003).
[14] H. B. Yu, Y. Luo, and K. Samwer, Adv. Mater. **25**, 5904 (2013).
[15] C. R. Cao, K. Q. Huang, N. J. Zhao, Y. T. Sun, H. Y. Bai, L. Gu, D. N. Zheng, and W. H. Wang, Appl. Phys. Lett. **105**, 011909 (2014).
[16] C. Rodríguez-Tinoco, M. Gonzalez-Silveira, J. Ràfols-Ribé, G. Garcia, and J. Rodríguez-Viejo, J. Non-Cryst. Solids **407**, 256 (2015).
[17] C. Rodríguez-Tinoco, M. Gonzalez-Silveira, J. Ràfols-Ribé, A. F. Lopeandía, M. T. Clavaguera-Mora, and J. Rodríguez-Viejo, J. Phys. Chem. B **118**, 10795 (2014).
[18] X. S. Li, W. W. Cai, J. An, S. Kim, J. Nah, D. X. Yang, R. Piner, A. Velamakanni, I. Jung, E. Tutuc, S. K. Banerjee, L. Colombo, and R. S. Ruoff, Science **324**, 1312 (2009).
[19] A. S. Pawbake, M. S. Pawar, S. R. Jadkar, and D. J. Late, Nanoscale **8**, 3008 (2016).
[20] S. Hussain, M. A. Shehzad, D. Vikraman, M. F. Khan, J. Singh, D.-C. Choi, Y. Seo, J. Eom, W.-G. Lee, and J. Jung, Nanoscale **8**, 4340 (2016).
[21] Z. Altounian, T. Guo-hua, and J. O. Strom-Olsen, J. Appl. Phys. **53**, 4755 (1982).
[22] Z. Altounian, E. Batalla, J. O. Strom-Olsen, and J. L. Walter, J. Appl. Phys. **61**, 149 (1987).
[23] B. S. Murty, D. H. Ping, K. Hono, and A. Inoue, Acta Mater. **48**, 3985 (2000).
[24] H. E. Kissinger, J. Res. Natl. Bur. Stand. **57**, 217 (1956).

[25] S. W. Lee, M. Y. Huh, E. Fleury, and J. C. Lee, Acta Mater. **54**, 349 (2006).
[26] L.-C. Zhang, J. Xu, and J. Eckert, J. Appl. Phys. **100**, 033514 (2006).
[27] J. C. Qiao and J. M. Pelletier, J. Non-Cryst. Solids **357**, 2590 (2011).
[28] P. Ramasamy, M. Stoica, A. H. Taghvaei, K. G. Prashanth, K. Ravi, and J. Eckert, J. Appl. Phys. **119**, 073908 (2016).
[29] S. Singh, M. D. Ediger, and J. J. de Pablo, Nat. Mater. **12**, 139 (2013).
[30] Y. Guo, A. Morozov, D. Schneider, J. W. Chung, C. Zhang, M. Waldmann, N. Yao, G. Fytas, C. B. Arnold, and R. D. Priestley, Nat. Mater. **11**, 337 (2012).
[31] L. Zhu, C. W. Brian, S. F. Swallen, P. T. Straus, M. D. Ediger, and L. Yu, Phys. Rev. Lett. **106**, 256103 (2011).
[32] R. Scott Smith, R. Alan May, and B. D. Kay, J. Phys. Chem. Lett. **6**, 3639 (2015).